Lubrication in refrigeration systems: numerical model for piston dynamics considering oil–refrigerant interaction

F P Grando[1,2], **M Priest**[1*], and **A T Prata**[2]
[1]Institute of Tribology, School of Mechanical Engineering, The University of Leeds, Leeds, UK
[2]Department of Mechanical Engineering, Federal University of Santa Catarina, Florianopolis, Brazil

The manuscript was received on 7 September 2005 and was accepted after revision for publication on 7 November 2005.

DOI: 10.1243/13506501JET147

Abstract: Piston dynamics plays a fundamental role in several processes related to the operation of hermetic reciprocating compressors used in refrigeration. For example, the refrigerant leakage through the radial clearance between piston and cylinder, which reduces compressor pumping efficiency, and also the viscous friction associated with the lubricant film in the radial clearance, which is related to energy consumption. It is important to optimize such variables, ensuring at the same time smooth operation of the piston in its reciprocating motion, minimizing wear and increasing lifetime.

In this context, numerical models studying piston dynamics provide a useful tool for engineering design. These models usually consider an oil film filling the piston–cylinder clearance and operating in the hydrodynamic regime. Determining cavitation conditions occurring along the ringless piston represents an additional difficulty in modelling. As refrigerant is present in the compressor environment, it inevitably interacts with the oil, changing lubricant characteristics. The refrigerant can dissolve in the oil at higher pressures, reducing viscosity, and can be released at lower pressures, leading to a two-phase flow.

This work explores how the interaction of oil and refrigerant affects piston dynamics, using a numerical model that considers as the lubricant a mixture of oil and refrigerant with variable properties. Comparing the results with simulations where pure oil is considered as the lubricant and a cavitation criterion is adopted, significant differences were observed in predicting piston trajectory and power consumption along the cycle.

Keywords: piston dynamics, oil–refrigerant mixture, two-phase flow, cavitation

1 INTRODUCTION

The tribological behaviour of the piston inside the cylinder bore has been recognized as an important factor influencing the performance of reciprocating machines. In addition to the main oscillatory movement performed by the piston, its behaviour also depends on small translations and rotations that can occur in the radial direction, where a clearance exists. These small movements are a consequence of the imbalance among the several forces and moments acting on the piston while it goes up and down during operation, shown in Fig. 1.

Given the importance of the oscillatory motions for the performance and reliability of reciprocating machines, all the major concerns in designing these systems, such as the gas leakage, frictional power loss, noise and wear, are tightly related to piston dynamics and lubrication, which also depend on the radial clearance. The dimension of this clearance involves a compromise between gas leakage and friction loss. If the radial clearance is too small, there will be considerable friction loss. On the other hand, larger clearances cannot prevent gas leakage.

Additionally, any contact between piston and cylinder has to be avoided, thus guaranteeing a

Corresponding author: Institute of Tribology, School of Mechanical Engineering, University of Leeds, Woodhouse Lane, Leeds LS2 9JT, UK. email: m.priest@leeds.ac.uk

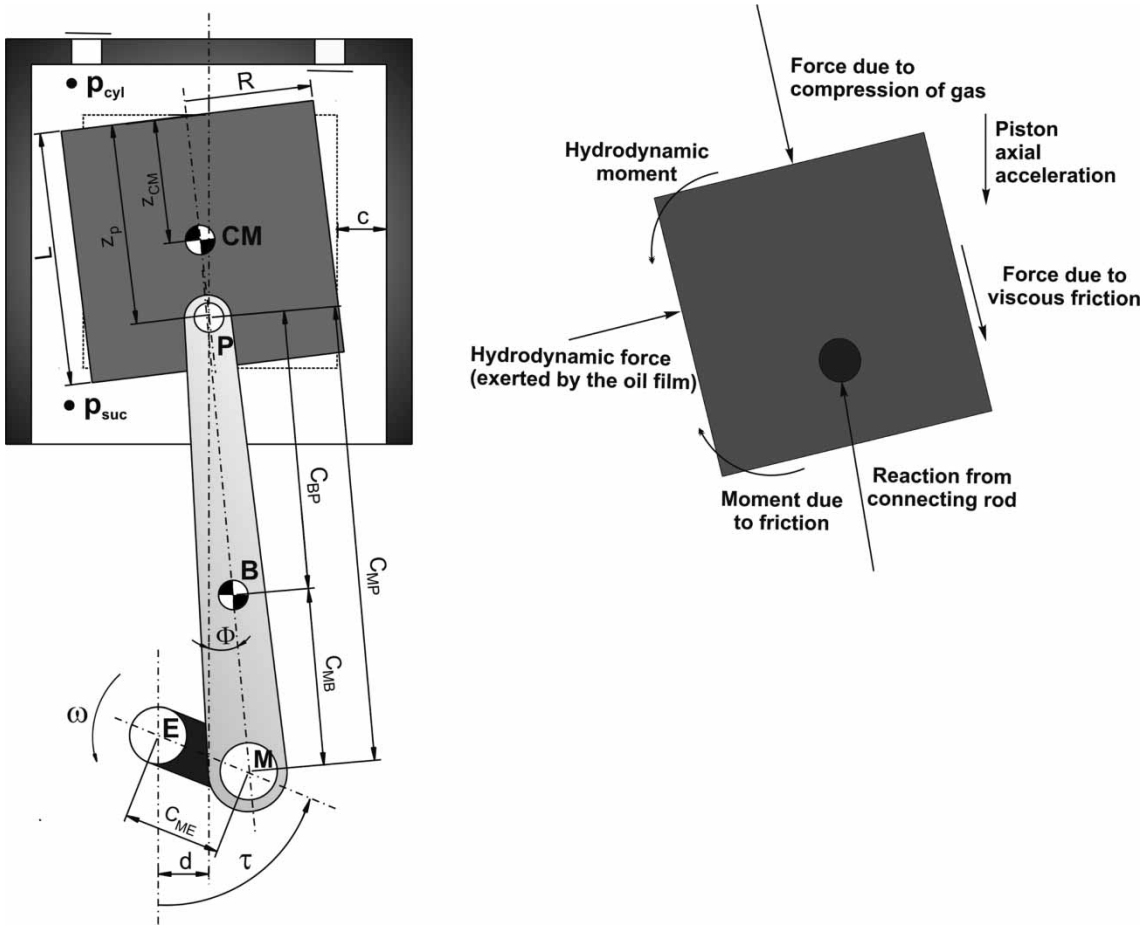

Fig. 1 Details of the piston–cylinder system and the main forces acting on the piston

stable motion and a reasonable piston life. Therefore, a thin fluid film between piston and cylinder should be maintained all times, which aims to ensure a hydrodynamic lubrication regime. However, boundary lubrication often occurs at top and bottom dead centres, as well as during starting and stopping. Such condition is crucial in studying piston ring lubrication, but is also observed for piston skirts, whether rings are present or not.

For those reasons, lubrication plays a fundamental role in performing the dynamic analysis of pistons in reciprocating motion. Several authors have been working towards this purpose. The first scientific investigations concerning piston dynamics started during the 1950s in Germany and in Britain, both from theoretical and experimental points of view [**1**], mainly dealing with diesel engines.

Repàci [**1**] developed a numerical model to simulate the behaviour of a piston in a diesel engine. Pressure was obtained analytically and two equations were used to determine piston velocity and acceleration: the balance of forces along the direction perpendicular to the connecting rod, and the moment equation around the wrist pin. Both equations were integrated by a Runge–Kutta method. His main attention was the impact of the piston against the cylinder bore, which is commonly called piston slap, and a good agreement with experimental results from the literature was reported.

Zhu *et al.* [**2**, **3**] have also confirmed the importance of the radial clearance and oil viscosity to the radial motion of the piston and its power consumption. They developed a numerical model for piston motion, lubrication, and friction in mixed lubrication. The proposed model was applied to an automotive engine and showed that hydrodynamic lubrication can improve piston life by reducing its wear and also reduces frictional loss.

Chittenden and Priest [**4**] proposed a model to calculate numerically the translation of the piston and its rotation around the gudgeon pin, considering the axial forces due to gas compression and connecting rod action, the inertia of the piston and the hydrodynamic forces of the lubricant film, considering the possibility of contact between piston and cylinder. Using the predictions of this model, Gamble *et al.* [**5**] calculated piston ring pack gas flow, dynamics and lubrication, showing significant

influence of piston motion on gas flow and inter-ring pressures. These changes can potentially affect oil film thickness, friction, wear and oil transport and degradation during engine operation. Further research also confirmed that the proposed numerical model presents better agreement with experimental results compared with the friction calculated, considering only axial piston movement along the cylinder axis [**6**].

Concerning small reciprocating compressors used in refrigeration, Prata *et al.* [**7**] developed the first model describing piston trajectory during its oscillatory movement inside the cylinder in a hermetic reciprocating compressor. Pressure was obtained via a finite volume solution of Reynolds equation, and the piston dynamics was solved using a Newton–Raphson procedure, obtaining radial velocities at the top and at the bottom of the piston.

Rigola *et al.* [**8**] included a similar numerical model in the simulation of thermal and fluid dynamic behaviour of hermetic reciprocating compressors. With additional information from experimental results for the compressor (motor torque and system pressures), preliminary results of forces and moments in the piston, connecting rod, and crankshaft were obtained.

Given the small clearances characteristic of this system, further research analysed the hypothesis of non-deformation of piston and cylinder [**9**]. Under severe conditions, results indicated that flexibility of the structure can produce variations of around 10 per cent in the initial system clearance and should be considered.

Despite the additional developments in the numerical modelling of the piston dynamics, there is still controversy regarding the cavitation criterion to be considered and the determination of gas leakage through the clearance. One possible reason for this is that all the previous works have not considered the interaction between the oil and the environment in which it operates, i.e., the solubility between oil and refrigerant in the case of refrigeration compressors.

The hermetic compressor environment is pressurized by the presence of refrigerant in the gas phase inside the shell, where the oil sump is located. In addition, refrigerant is being compressed inside the cylinder, whose walls present a thin lubricant film. Inevitably interaction occurs between oil and refrigerant, affecting system operation. A series of experimental studies have dealt with the performance of lubricant in a pressurized refrigerant environment. Considerable reduction in film forming capability was observed as the environment pressure increases [**10**, **11**]. The study of wear performance also showed that combinations of lubricant and refrigerant with lower viscosities are subjected to more severe conditions and even boundary lubrication [**12**, **13**]. The results of these studies highlight effects such as the reduction of lubricant viscosity with refrigerant solubility and the increase in solubility with pressure.

Other effects can also be observed in addition to changes in liquid properties. Under significant negative pressure gradients, refrigerant can be released in the form of bubbles as solubility decreases, giving raise to a flashing flow, where liquid–vapour phase change occurs. Experimental tests in straight horizontal pipes have shown that considerable outgassing occurs with the decrease of pressure along the flow, and even foaming characteristics can be seen when larger amounts of gas are released [**14**, **15**]. In the light of these findings, the first numerical models were proposed by Grando and Prata [**16**] and Barbosa *et al.* [**17**], both obtaining good agreement with experimental results from Lacerda *et al.* [**14**].

Such developments are useful to the analysis of lubrication and leakage processes inside the compressor. The amount of gas released in the flow can be related to the leakage of refrigerant, which consequently influences pumping efficiency. The understanding of mixture properties and flashing flows creates an appropriate opportunity to advance in the study of cavitation. This phenomenon has long been associated with the interaction of the oil, and gases present in the working environment. Many researchers explicitly mention terms referring to the solubility between oil and ambient gases, commonly attributing the break of liquid film continuity to the release of gas when the 'saturation pressure' is reached [**18**]. This situation can be identified for the compressor operation when refrigerant is released from the oil, representing an alternative to the usual methodologies that use intermediate boundary conditions to model cavitation.

The current authors have proposed a numerical two-phase model considering cavitation from the release of gas and explored it in the study of partial journal bearings, where the difference between modelling considering pure oil or oil–refrigerant as the lubricant was discussed [**19**]. The model was also applied to long journal bearings. Under the presence of gas, it was seen that classical boundary conditions used to determine cavitation produced results significantly different than those obtained using the two-phase methodology [**20**].

The present work continues to explore the model proposed, introducing, for the first time, the two-phase methodology to study the problem of piston dynamics in the refrigeration compressor. To determine the secondary motion of the piston, the analysis of the thin lubricant film considers the behaviour of the fluid mixture along the flow, evaluating the dissolution of the gas in the oil and the interaction

between liquid and gas phases, thereby changing lubricant properties. Differences compared with the methodologies considering constant properties and common cavitation criteria are highlighted.

2 PROBLEM FORMULATION

A typical piston–cylinder system for small reciprocating compressors is presented in Fig. 1. The piston (length L and a constant radius R throughout the length) is driven in a reciprocating motion by the action of a crankshaft on the connecting rod. Apart from the presence of intermediate recesses, this profile is a good approximation of a piston for domestic refrigeration compressors and also attends the aims of this preliminary work. A full cycle occurs for each 360° of rotation of the crankshaft, assumed to start at $\tau = 0°$ when the piston is near the bottom dead centre. An offset d exists between the cylinder axis and the crankshaft centre.

The piston is subjected to a gas force due to the pressure difference between the compression chamber and the shell. While the pressure inside the cylinder (p_{cyl}) varies with the movement, the compression suction pressure (the pressure in the compressor shell, p_{suc}) is assumed constant.

A complete fluid film exists within the clearance either during the upstroke or downstroke movement. For the first, lubricant is carried to the chamber due to the piston movement. The lubricant present inside the cylinder interacts with the refrigerant being compressed. During the downstroke, the lubricant is now brought out of the cylinder with the piston axial motion. Through this process, refrigerant that has been dissolved into the oil escapes from the cylinder, reducing pumping efficiency. Such lubricant feeding conditions occur because of the compressor assembly, which uses a small piston–cylinder clearance to sealing the compression chamber. In addition, compressor operation also ensures that lubricant is abundantly splashed at cylinder walls, piston base, and the gudgeon pin. Furthermore, for the downstroke condition, small droplets of oil that have been also carried into the cylinder during the suction of refrigerant from the shell environment assures that fully flooded lubrication can be assumed [**7**].

At any time during the cycle, refrigerant is dissolved to a certain amount in the oil and can potentially be released in the form of bubbles when the saturation pressure is reached. Determination of the dissolved refrigerant is a difficult task, especially as the process undergoes a rapid transient. Despite some preliminary research on the transient absorption of refrigerant in the oil [**21**, **22**], this issue is not completely resolved and different absorption estimates are tested in this work. It is additionally assumed that the oil splashed at the bottom of the piston is in equilibrium with the refrigerant present in the shell, therefore resulting in a saturated mixture at p_{suc}.

The lubricant film responds hydrodynamically to the imbalance of the other forces acting on the piston and influences the rotation and translation of the component in its secondary motion. To characterize this movement, several coordinate systems could be used. A very convenient one is that where eccentricities at top and bottom of the piston are calculated, from which all the others can be determined if a rigid piston is assumed. Positioning of these eccentricities (e_t and e_b) is presented in Fig. 2. All the movements are assumed to occur in the plane perpendicular to the wrist pin axis.

Figure 2 also shows the coordinate systems adopted in the solution of the problem. A Cartesian system xyz is used to calculate the balance of forces. The vertical axis z coincides with the cylinder axis and x indicates the other direction of movement. In addition, a cylindrical system $r\theta\gamma$ positioned at the top of the piston is convenient to calculate hydrodynamic film pressures throughout the radial clearance. This system moves with the axial velocity of the piston, V_P.

In this context, with simultaneous solution of the pressure in the lubricant film and the balance of forces in the component, the piston trajectory throughout the cycle can be characterized.

2.1 Mathematical modelling

For the piston–cylinder system, most of the basic assumptions adopted in hydrodynamic lubrication

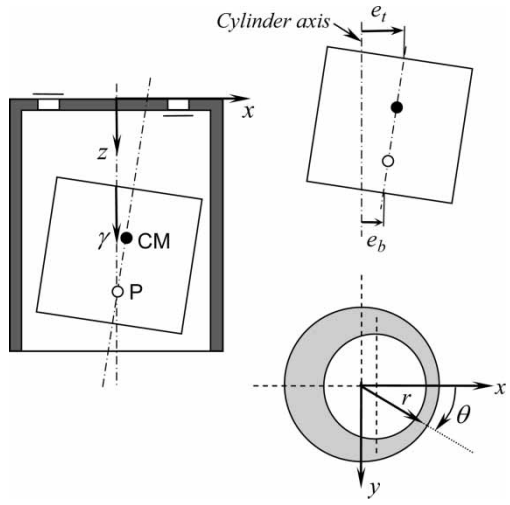

Fig. 2 Coordinate systems and variables used to characterise the secondary movement

problems remain valid [**23**], such as the negligible variation of pressure in the radial direction and laminar flow.

However, the problem now considers the variation of fluid properties due to the interaction of oil and refrigerant, and particularly the two-phase flow occurring when gas is released. To characterize fractional composition of refrigerant and oil in the liquid mixture, as well as the proportion of liquid and gas in the two-phase flow, a series of parameters are needed, defined as follows.

Refrigerant mass fraction: the amount of refrigerant dissolved in the liquid mixture, on a mass basis, defined by equation (1)

$$w = \frac{m_{\mathrm{lr}}}{m_{\mathrm{l}}} \tag{1}$$

The maximum quantity of refrigerant that can be dissolved in the liquid for a specific condition of pressure and temperature is defined as the solubility

$$w_{\mathrm{sat}} = w_{\mathrm{sat}}(p, T) \tag{2}$$

Quality: the ratio between the mass of gas and the total mass of the mixture within a cross-sectional area of the flow. In terms of the refrigerant mass fraction, it can be related to the overall fluid composition at a given instant, thus being given by

$$\chi = \frac{w_{\mathrm{o}} - w}{\mathrm{I} - w} \tag{3}$$

The overall fluid composition, w_{o}, varies with the piston position. When lubricant flows into the cylinder, it is the saturation value for the mixture at the shell pressure, p_{suc}. For the downstroke movement, w_{o} can be estimated from the pressure inside the cylinder. However, as the piston moves at considerable speeds, the refrigerant may not be able to dissolve to its maximum in the oil. As the precise value is not known, intermediate values will be estimated from the mass fraction at the previous time (w_{r}) according to equation (4)

$$w_{\mathrm{o}} = w_{\mathrm{r}} + \kappa[w_{\mathrm{sat}}(p_{\mathrm{cyl}}, T) - w_{\mathrm{r}}] \tag{4}$$

Additional assumptions are required regarding release and absorption of gas in the flow within the clearance that determines the refrigerant mass fraction w_{r}. In this case, it is considered that the gas is released instantaneously when the saturation pressure is reached. However, the gas is not reabsorbed in the liquid if film pressure increases. Further discussion of this assumption can be found in reference [**19**, **20**].

In addition to the mass-related parameters, the ratio between the gas volume and the total volume within a section of the flow is also required. This is defined as the void fraction, which for identical velocities of both phases is determined by

$$\phi = \frac{1}{(1 + ((1/\chi) - 1)\rho_{\mathrm{g}}/\rho_{\mathrm{l}})} \tag{5}$$

As previous research shows [**14**, **15**], assuming similar velocities is a reasonable approach for the two-phase flow of oil and refrigerant mixtures. For this particular condition, a homogeneous two-phase flow model can be adopted, where the liquid–gas mixture can be replaced by a monophasic pseudofluid, whose density and viscosity are given by reference [**24**]

$$\bar{\rho} = \phi\rho_{\mathrm{g}} + (1 - \phi)\rho_{\mathrm{l}} \tag{6}$$

and

$$\bar{\mu} = \chi\mu_{\mathrm{g}} + (1 - \chi)\mu_{\mathrm{l}} \tag{7}$$

Having defined the characteristics of the lubricant, the governing equation for the lubrication of the piston–cylinder clearance can be written. Considering pressure and viscous forces to be dominant, the flow is governed by the Reynolds equation, where the homogeneous properties are considered as presented in equation (8)

$$\frac{\partial}{\partial\theta}\left(\frac{\bar{\rho}h^3}{12\bar{\mu}R^2}\frac{\partial p}{\partial\theta}\right) + \frac{\partial}{\partial\xi}\left(\frac{\bar{\rho}h^3}{12\bar{\mu}R^2}\frac{\partial p}{\partial\xi}\right) = \frac{V_p}{2R}\frac{\partial(\bar{\rho}h)}{\partial\xi} - \frac{\partial(\bar{\rho}h)}{\partial t} \tag{8}$$

For a given time, if the position and velocities resulting from the piston secondary motion are known, the governing equation can be solved considering the following boundary conditions

$$\begin{aligned} &\xi = 0 \longrightarrow p = p_{\mathrm{cyl}} \\ &\xi = \frac{R}{L} \longrightarrow p = p_{\mathrm{suc}} \\ &p(\theta = 0) = p(\theta = 2\pi) \end{aligned} \tag{9}$$

where no intermediate boundary conditions are required for the cavitation of the film as it is automatically determined from the release of gas. In conventional single-phase methodologies, these boundary conditions are also respected, but

additional assumptions on the behaviour of pressure for intermediate positions are required.

When determining the pressure field across the lubricant film, at the same time the balance of forces and moments in the piston must be satisfied. The main forces acting on the piston are the gas force, the connecting rod force, inertia effects, friction force, and the hydrodynamic force due to the lubricant film. Friction and hydrodynamic forces can also produce momentum around the wrist pin.

From the scheme previously shown in Fig. 1, the following equations can be written for the piston

$$\sum F_z = F_g + F_f + F_{rz} = mA_p \tag{10}$$

$$\sum F_x = F_h + F_{rx} = mc\omega^2\left(\ddot{\varepsilon}_t - z_{CM}\frac{\ddot{\varepsilon}_t\ddot{\varepsilon}_b}{L}\right) \tag{11}$$

$$\sum M_{pin} = M_h + M_f = I_P c\omega^2\frac{\ddot{\varepsilon}_t - \ddot{\varepsilon}_b}{L} \tag{12}$$

The forces and moments acting on the piston related to the hydrodynamic force due to the lubricant film and to the viscous frictional force can be determined from the pressure profile as follows

$$F_h = -\int_0^L\int_0^{2\pi} p(\theta,\xi)R^2\cos\theta\,\mathrm{d}\theta\,\mathrm{d}\xi \tag{13}$$

$$M_h = \int_0^L\int_0^L p(\theta,\xi)(z_p - R\xi)R^2\cos\theta\,\mathrm{d}\theta\,\mathrm{d}\xi \tag{14}$$

and

$$F_f = -\int_0^L\int_0^{2\pi}\left(\frac{h}{2R}\frac{\partial p}{\partial\xi} + \mu\frac{V_p}{h}\right)R^2\,\mathrm{d}\theta\,\mathrm{d}\xi \tag{15}$$

$$M_f = -\int_0^L\int_0^{2\pi}\left(\frac{h}{2R}\frac{\partial p}{\partial\xi} + \mu\frac{V_P}{h}\right)R^3\cos\theta\,\mathrm{d}\theta\,\mathrm{d}\xi \tag{16}$$

The force of gas can be easily calculated by

$$F_g = \pi R^2(p_{cyl} - p_{suc}) \tag{17}$$

Connecting rod forces are obtained from the respective balance of forces and moments in this component. These equations also consider the reactions in the crankshaft, which can be determined analytically from the geometry of the system. Analytical expressions for piston acceleration and velocity are derived similarly. Details of these manipulations can be found in Prata *et al.* [**7**].

As previously stated, for a given time, if the characteristics of the secondary movement of the piston are known, equations (8) and (10) to (12) are satisfied. However, the inverse problem is the one of interest, so that piston conditions are not initially known. Therefore, a solution procedure to solve simultaneously pressure and dynamics is required. Details of the methodology adopted in this work are presented subsequently.

2.2 Solution methodology

From the input of connecting rod dynamics, equation (10) can be used to determine F_{rx}. Therefore, for each crankshaft angle τ, piston trajectory can be determined from equations (11) and (12) that implicitly depend on ε_t and ε_b. In these equations, however, knowledge of the pressure profile is required to determine forces and moments related to the hydrodynamic fluid film.

To this end, solution starts from initial estimates for piston eccentricities and velocities for the initial crankshaft angle

$$\varepsilon_t^0,\ \varepsilon_t^0,\ \dot{\varepsilon}_t^0,\ \dot{\varepsilon}_t^0 \quad \text{for } \tau = 0 \tag{18}$$

As the piston presents a periodical trajectory, the converged solution does not depend on the initial guess.

Using these values, time is advanced in a time step to $\tau + \Delta\tau$ and an iterative process is used to search for the correct values for radial velocities that satisfy the balance of forces. In this work, a Newton–Raphson procedure is adopted [**8**]. Piston eccentricities and accelerations are determined from

$$\varepsilon_t^{\tau+\Delta\tau} = \varepsilon_t^\tau + \dot{\varepsilon}_t^{\tau+\Delta\tau}\cdot\Delta\tau, \quad \varepsilon_b^{\tau+\Delta\tau} = \varepsilon_b^\tau + \dot{\varepsilon}_t^{\tau+\Delta\tau}\cdot\Delta\tau \tag{19}$$

$$\ddot{\varepsilon}_t^{\tau+\Delta\tau} = \frac{\dot{\varepsilon}_\tau^{\tau+\Delta\tau} - \dot{\varepsilon}_t^\tau}{\Delta\tau}, \quad \ddot{\varepsilon}_b^{\tau+\Delta\tau} = \frac{\dot{\Delta}_b^{\tau+\Delta\tau} - \dot{\varepsilon}_b^\tau}{\Delta\tau} \tag{20}$$

To determine the forces acting on the piston, pressure is solved from Reynolds equation (8), with the film thickness calculated with values for ε_t and ε_b. Then, the equation is numerically integrated using a finite volumes approach [**25**], where the whole extent of the lubricant film is discretized. It should be noted that the density and viscosity depend on pressure, so that an iterative process is also required to solve the pressure field.

When a converged solution is obtained for $\tau + \Delta\tau$, another advance in the time step is performed and the procedure is repeated, marching in time until a periodical solution is found for the whole cycle.

The solution algorithm is schematically represented in Fig. 3.

3 RESULTS AND DISCUSSION

The proposed methodology has been used to simulate dynamics for a pre-defined piston–cylinder

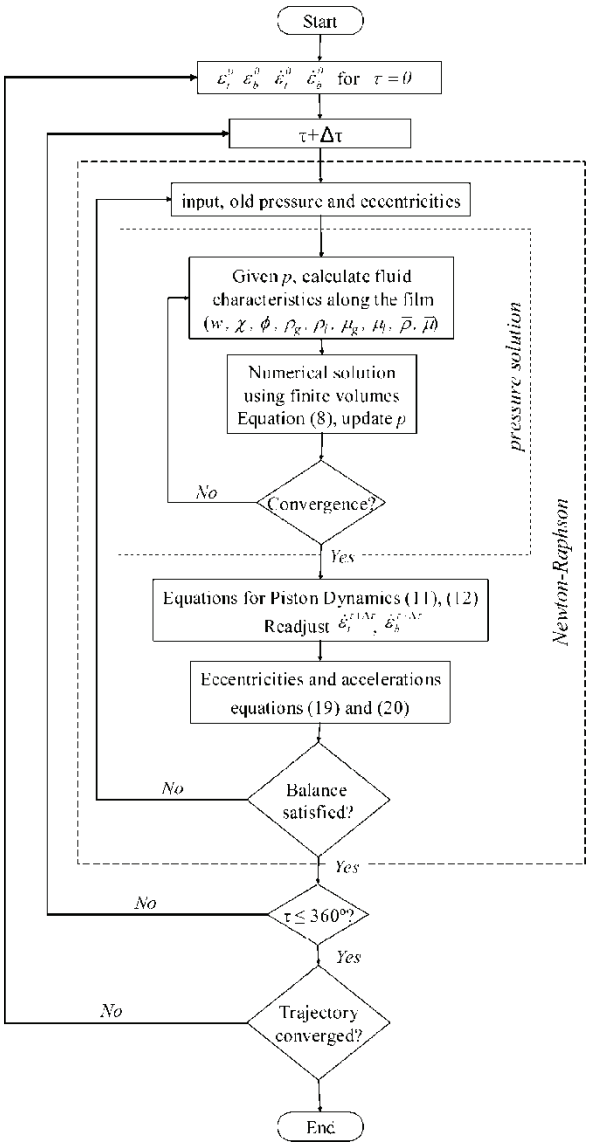

Fig. 3 Algorithm employed for the numerical methodology

system. A combination of a synthetic oil and a hydrofluorocarbon (HFC) refrigerant commonly adopted in domestic refrigeration compressors was considered. The properties for a mixture of the refrigerant HFC-134a and polyol ester EMKARATE RL10H were provided by the oil manufacturer and adjusted by curve fitting. Correlations used are presented in Appendix 2. For simplicity, the fluid is assumed to be at constant temperature.

Relevant compressor data required for the simulation is presented in Table 1, as well as the parameters defined for the numerical simulation.

In addition, pressure in the cylinder as a function of the crankshaft angle is required. Figure 4 graphically sketches this variation, which can also be compared to the shell pressure, assumed constant. Pressure in the cylinder can either be obtained

Table 1 Geometry and numerical data used in the simulations

	Parameter	Value
Geometry	R (mm)	10.5
	L (mm)	21.0
	c (μm)	5.0
	z_P (mm)	12.08
	z_{CM} (mm)	9.53
	C_{BP} (mm)	25.54
	C_{MP} (mm)	36.47
	d (mm)	2.0
	ω (rad/s)	370
	m (g)	34.6
	m_b (g)	24.2
	I_P (kg m^2)	0.287×10^{-5}
	p_{suc} (kPa)	238.50
	T (°C)	60
Numerical	Mesh (θ, ξ)	18×30
	$\Delta\tau$ (°)	5
	Tolerance (p)	1×10^{-6}
	Tolerance (ε_i)	1×10^{-4}

from numerical simulation of the compression cycle or be measured experimentally [**26**].

Referring to equation (4), two different absorption conditions were tested: the first simulated a low absorption condition ($\kappa = 0.05$), whereas the second ($\kappa = 0.50$) indicates easy dissolution of the refrigerant in the oil even at fast transients. The latter dissolves twice as much refrigerant as the former, which indicates a lower viscosity of the lubricant in such conditions, as well as a higher potential to release gas under negative pressure gradients, related to a higher saturation pressure. However, at lower coefficient of absorption refrigerant dissolves for a longer time.

Results of the two-phase model are compared to those obtained using classical methodologies, for a single-phase fluid. Different cavitation criteria are also used. Table 2 summarises the cases analysed in addition to the two-phase flow model.

The methodology requires only minor changes to incorporate the additional single-phase cases. To consider constant properties, the algorithm will not readjust them during the iterative process. Therefore, referring to Fig. 3, in the pressure solution stage, only the numerical solution for pressure, equation (8), is required. In addition, when a cavitation condition is considered, a routine to verify pressures is included. This basically requires that, if during the solution of the linear system a value below the cavitation pressure was obtained, it is replaced by the cavitation pressure. This procedure, along with an iterative solution for the linear system (e.g. CTDMA [**25**]), is the commonly adopted cavitation algorithm [**27**]. The three different criteria compared in this work with the two-phase flow modelling are characterized as follows.

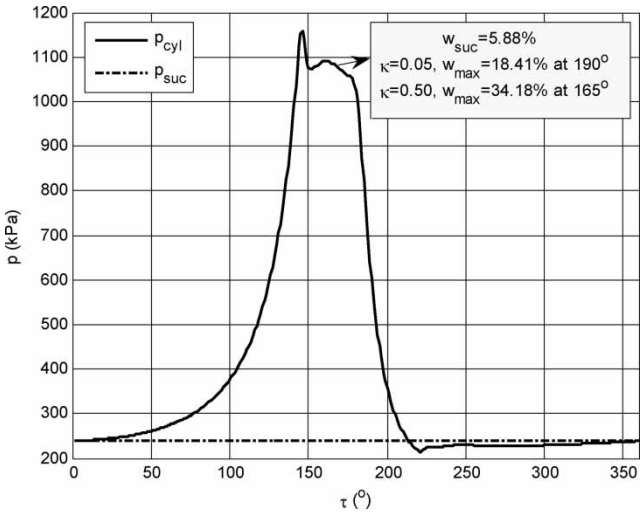

Fig. 4 Pressures in the cylinder and shell during operation and mixture characteristics

1. NCav: in this case, no cavitation pressure is assumed, i.e., the pressure is always that determined by the solution of the linear system. This criterion in nothing else than the Sommerfeld condition.
2. Cav: the cavitation pressure is assumed to vary linearly along the length of the piston, starting from the cylinder pressure at the top (p_{cyl}) and reaching the shell pressure at the bottom of the piston (p_{suc}). Whenever the pressure calculated from a given position is less than the cavitation pressure at that position, the former value is replaced by the latter.
3. Cav_{min}: the minimum value between cylinder and shell pressures is considered as a constant value for the cavitation pressure. When the value calculated is smaller than this minimum value, it is updated to the cavitation pressure.

Table 2 Different conditions explored

Fluid	Case	Cavitation criterion	μ (mPa s)
Oil	Oil NCav	None (Sommerfeld)	4.9481
	Oil Cav	Linear variation between p_{cyl} and p_{suc}	
	Oil Cav_{min}	Constant, minimum between p_{cyl} and p_{suc}	
Oil–refrigerant (saturated at p_{suc})	OR NCav	None (Sommerfeld)	4.2514
	OR Cav	Linear variation between p_{cyl} and p_{suc}	
	OR Cav_{min}	Constant, minimum between p_{cyl} and p_{suc}	
Oil–refrigerant	$2p_{05}$	Automatically determined from w_{sat}	Variable
Two-phase	$2p_{50}$		

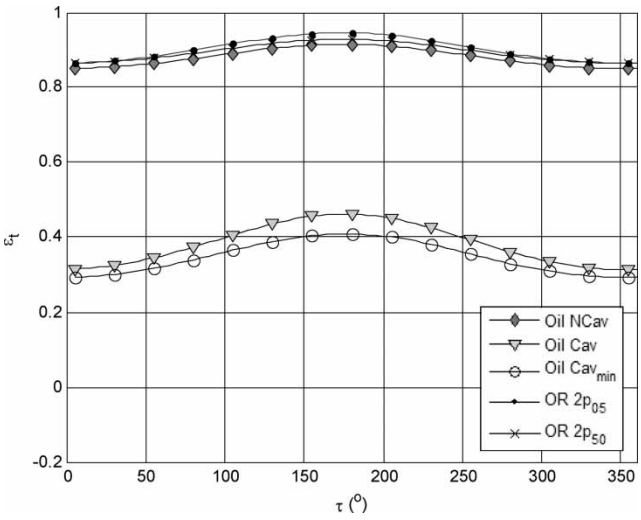

Fig. 5 Eccentricity at the top of the piston

Figure 5 presents the eccentricity for the top of the piston as a function of the crankshaft angle. Differences simply due to the lubricant viscosity, i.e. Oil NCav versus OR NCav, etc., were not shown to be significant. Thus, for clarity, results for oil–refrigerant single phase are omitted. However, the cavitation criteria adopted showed to be crucial in determining the trajectory. Higher eccentricities are observed when cavitation is not considered, whereas the top of the piston moves closer to the cylinder axis when cavitation criteria are adopted. The two-phase model results were similar to those neglecting cavitation. An increase in the eccentricity at the top is observed for the mixture absorbing a less amount of refrigerant (OR $2p_{05}$).

The behaviour of the piston is explained if Fig. 6 is analysed simultaneously with Fig. 5. Individually, the conclusions from the top of the piston can be drawn.

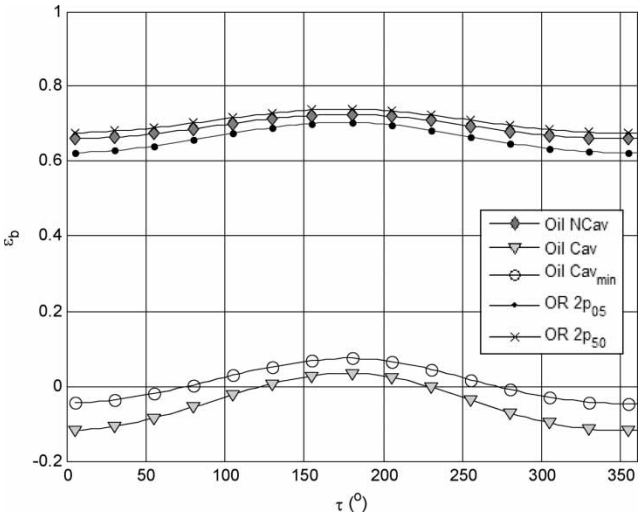

Fig. 6 Eccentricity at the bottom of the piston

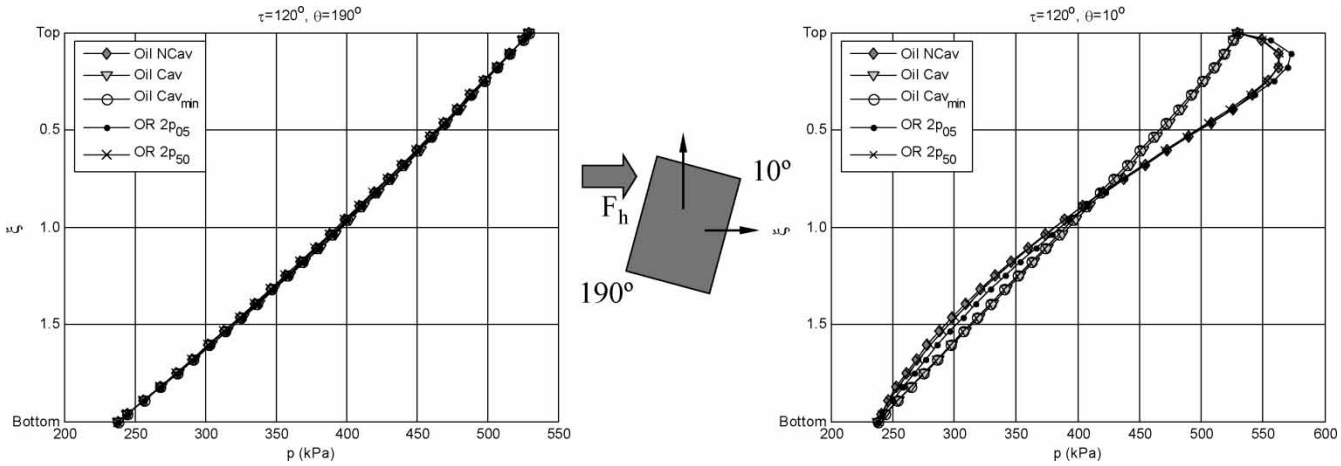

Fig. 7 Pressures for two opposite sides of the piston at $\tau = 120^\circ$

However, it can be noticed a greater amplitude of the movements for the results where cavitation criteria was adopted, indicating additional effort from the piston to balance the forces along the cycle. Along with the more inclined condition in which the piston moves, a hydrodynamic wedge effect is expected to balance the forces. On the other hand, the two-phase model has predicted a more stable motion, as also observed for the non-cavitated solution. For the piston lubricated with the less absorbent mixture, inclination slightly increases at the top dead centre region.

To evaluate deeper the differences in eccentricity, an analysis of pressure profiles along the piston trajectory was made. In Fig. 7, the profiles for circumferential positions $\theta = 10^\circ$ and $\theta = 190^\circ$ are presented for a crankshaft angle $\tau = 120^\circ$. Such circumferential positions are chosen among the discretized points for being the closest to thrust and anti-thrust surfaces of the piston, respectively. At this time, the piston is moving upwards. Owing to the high axial velocity, a significant wedge effect develops in the anti-thrust surface of piston, and hydrodynamic forces act pushing the piston against the wall at $\theta = 0^\circ$.

The two-phase flow model presents limited difference in this region, as the lubricant flows against a positive pressure gradient. Therefore, no release of gas takes place in the upward movement of the piston.

However, a different picture occurs for the piston returning to the bottom dead centre. Initially, a negative pressure gradient develops and a divergent gap exists for the flow along the minimum film thickness region ($\theta = 0^\circ$). Such a situation can be seen in Fig. 8, for a crankshaft angle of 240°. As the fluid reaches the divergent region, pressure tends to decrease and refrigerant is released from the oil, giving rise to a two-phase flow with further expansion of the gas to accommodate changes in geometry. As the shell pressure at the bottom of the piston is communicated, pressure recovery also takes place. The

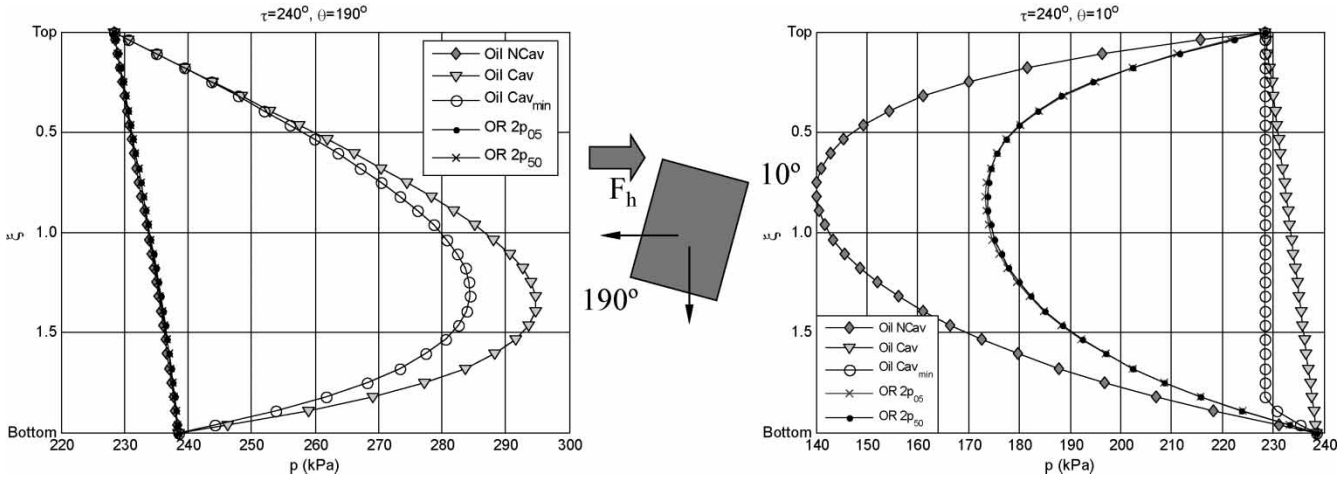

Fig. 8 Pressures for two opposite sides of the piston at $\tau = 240$

Table 3 Cycle averaged values for power consumption due to viscous friction

Case	P_{ot} (W)
Oil NCav	6.904
Oil Cav	4.249
Oil Cav_{min}	4.240
OR NCav	5.941
OR Cav	3.663
OR Cav_{min}	3.652
$2p_{05}$	5.960
$2p_{50}$	6.189

effect of gas expansion is clear when comparing the results with those for a non-cavitated condition. On the other hand, when a cavitation criterion is applied, the behaviour is exactly the opposite. The low pressures cause the rupture of the film, and a squeeze film effect provokes increase in pressure at $\theta = 190^\circ$, eventually resulting in the same effect on the piston.

As an important parameter for piston design, power consumption was also determined. After calculating the friction force using equation (15), power loss due to viscous friction can be averaged for the whole cycle as

$$P_{ot} = \frac{1}{2\pi}\int_0^{2\pi} F_f \cdot V_P \, d\tau \tag{21}$$

Values are presented in Table 3, where it can be seen that lower values are obtained when cavitation is artificially considered, as the cavitated points are removed from calculation (negligible shear stress). Here, viscosity plays a major role and when the oil–refrigerant is considered as the lubricant, lower values are obtained. Results for the two-phase flow model are closer to that for the oil–refrigerant lubricant disconsidering cavitation, although slightly higher. One of the reasons is that, when gas is released from the lubricant, the viscosity will actually increase as a result of a lower mass fraction of refrigerant and despite the presence of gas with lower viscosity. The correlation to calculate the viscosity of the oil–refrigerant liquid mixture is presented in Appendix 2 and is referred to this analysis. Minimal differences occur for the different mixture conditions, with higher friction for the mixture with more refrigerant dissolved, despite its lower viscosity.

Finally, the leakage of oil can also be estimated from the pressure profile determined. At the bottom of the piston, it is calculated as

$$q_{bottom} = \int_0^{2\pi} \left(-\frac{h^3}{12\bar{\mu}R}\frac{\partial p}{\partial \xi} + V_P \frac{h}{2} \right)\Bigg|_{z=L} R \, d\theta \tag{22}$$

Figure 9 presents results for flow rate. The main effect has been proved to be the axial movement of the piston (qVp), with only small differences between

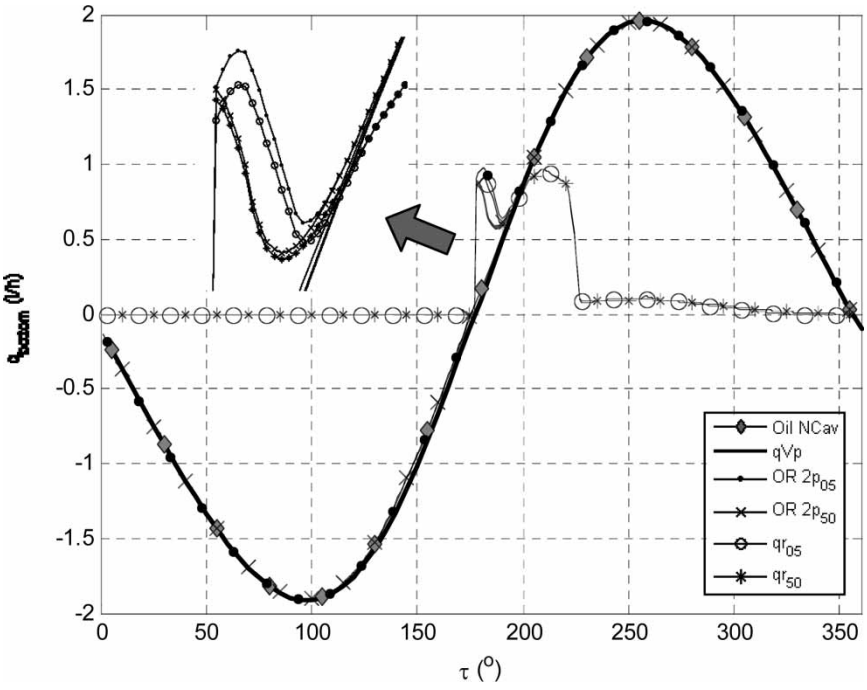

Fig. 9 Volumetric flow rate along the cycle and the participation of gas refrigerant for each two-phase case

the cases. This indicates the sealing capacity promoted by the small clearance. This value is significant for any of the single phase simulations, but an opportunity to estimate the leakage of refrigerant as gas can also be performed using the two-phase model, estimating such leakage from equation (5) with the void fraction of the liquid–gas lubricant leaving the piston skirt. This result is also presented. Refrigerant flow starts a little before 180°, when the piston changes direction; the presence of gas naturally increases the volumetric flow rate. The discontinuity results from the assumption that reverse flow starts with the change in direction of the piston. Therefore, a delay in the reverse flow is suggested, which is currently not predicted. Additional refinements will be required as pressure flow is conceivably important for that region. Nevertheless, it can be seen that maximum leakage occurs for the lowest piston velocities, as no resistence is imposed against the pressure gradient and the mixture presents has a high mass fraction. Thereafter, gas leakage gradually reduces as pressure in the cylinder starts to decrease, reducing the amount of refrigerant dissolved. A small difference can be observed as a result of the different absorption characteristics of the mixtures. Surprisingly, the mixture with a lower mass fraction presents a higher leakage than the one capable of absorbing more refrigerant, as can be seen in detail in Fig. 9. This is actually the reason to this behaviour: while the mixture with a higher coefficient of absorption has too much refrigerant dissolved from the start, as pressure decreases refrigerant is released as soon as cylinder pressure decreases. On the other hand, the mixture with lower coefficient of absorption can still absorb refrigerant; despite pressure decreases, levels are high and the refrigerant remains dissolving in the oil, therefore being carried out of the compression chamber. It should be stressed that the results intend to show the prediction capability of the model, although significant advances are required to the precise determination of the oil–refrigerant mixture inside the cylinder, thereby improving the understanding of the refrigerant release during suction.

4 CONCLUSIONS

A model considering the interaction of the oil and refrigerant during piston operation has been proposed. The model advances previous solutions available by including the variation of properties during the cycle. The change in properties is a result of the dissolution of the refrigerant in the oil and its release throughout the piston–cylinder clearance when negative pressure gradients are experienced.

1. Compared to the previous solutions considering pure oil with constant properties, small differences are observed in relation to non-cavitated conditions, and no agreement was found with cavitated solutions. This highlights the controversy regarding cavitation boundary conditions, as considerable discrepancy was observed.
2. The model predicts power consumption similarly to the single-phase model considering oil–refrigerant viscosity. Using cavitation criteria, a much lower value was predicted.
3. Differences in the oil leakage through the clearance during downstroke were not significant for most of the cycle, but close to the top dead centre the two-phase model predicts higher volumetric leakage. The model can estimate the amount of refrigerant released as gas with the oil, having calculated the volume ratio of the phases during pressure solution.
4. The influence of the coefficient of absorption in the mixture behaviour was not significant, although at lower rates of absorption a higher leakage was predicted. Nevertheless, additional studies to understand the transient behaviour of the oil–refrigerant mixture are crucial to the advances of the present model. Simultaneously, future work shall consider also a better estimate for the flow of oil close to the top dead centre, potentially the instant where maximum refrigerant leakage occurs.

Applying the model to more realistic geometries of the piston is also relevant. For instance, in recesses, where the clearance increases, the two-phase flow model is capable of predicting release of gas even during the upstroke, which may significantly affect piston trajectory.

ACKNOWLEDGEMENTS

This research was supported financially by the Programme Alβan, the European Union Programme of High Level Scholarships for Latin America, identification number E03D22219BR. Assistance from the Brazilian Compressor Company EMBRACO SA is also acknowledged.

REFERENCES

1 **Repàci, A.** Non linear modelling of the piston slap phenomenon in an alternative internal combustion engine. *Math. Model.*, 1987, **8**, 366–367.
2 **Zhu, D., Cheng, H. S., Takayuki, A.,** and **Hasmai, K.** A numerical analysis for piston skirt in mixed lubrication – Part I: basic modelling. *J. Tribol.*, 1992, **114**, 553–562.

3 **Zhu, D., Cheng, H. S., Takayuki, A.,** and **Hasmai, K.** A numerical analysis for piston skirt in mixed lubrication – Part II: deformations considerations. *J. Tribol.*, 1993, **115**, 125–133.

4 **Chittenden, R. J.** and **Priest, M.** Analysis of the piston assembly, bore distortion and future developments. *Tribol. Ser.*, 1993, **26**, 241–270.

5 **Gamble, R., Priest, M., Chittenden, R. J.,** and **Taylor, C. M.** Preliminary study of the influence of piston secondary motion on piston ring lubrication. *Tribol. Ser.*, 2000, **38**, 679–691.

6 **Mufti, R. A.** *Total and component friction in a motored and firing engine*. PhD Thesis, University of Leeds, Leeds, 2004.

7 **Prata, A. T., Fernandes, J. R. S.,** and **Fagotti, F.** Dynamic analysis of piston secondary motion for small reciprocating compressors. *J. Tribol.*, 2000, **122**, 752–760.

8 **Rigola, J., Perez-Segarra, C. D.,** and **Oliva, A.** Numerical simulation of the leakage through the radial clearance between piston and cylinder in hermetic reciprocating compressors. Proceedings of the International Conference of *Compressors and their systems*, London, UK, 2003, pp. 313–321.

9 **Cho, J. R.** and **Moon, S. J.** A numerical analysis of the interaction between the piston oil film and the component deformation in a reciprocating compressor. *Tribol. Int.*, 2005, **38**(5), 459–468.

10 **Akei, M., Mizuhara, K., Taki, T.,** and **Yamamoto, T.** Evaluation of film-forming capability of refrigeration lubricants in pressurized refrigerant atmosphere. *Wear*, 1996, **196**, 180–187.

11 **Na, B. C., Chun, K. J.,** and **Han, D. C.** A tribological study of refrigeration oils under HFC-134a environment. *Tribol. Int.*, 1997, **30**(9), 707–716.

12 **Safari, S.** and **Hadfield, M.** Wear behaviour of the piston/gudgeon pin in a hermetic compressor with replacement CFC refrigerants. *Wear*, 1998, **219**, 8–15.

13 **Ciantar, C., Hadfield, M., Smith, A. M.,** and **Swallow, A.** The influence of lubricant viscosity on the wear of hermetic compressor components in HFC-134a environments. *Wear*, 1999, **236**, 1–8.

14 **Lacerda, V. T., Prata, A. T.,** and **Fagotti, F.** Experimental characterisation of oil-refrigerant two-phase flow. Proceedings of the ASME – Advanced Energy Systems Division, 2000, vol. 40, pp. 101–109.

15 **Castro, H. O. S., Gasche, J. L.,** and **Conti, W. P.** Foam flow of oil-refrigerant R134a mixture in a small diameter tube. In Proceedings of the 10th International Refrigeration and Air Conditioning Conference at Purdue, Purdue, USA, 2004, paper R171.

16 **Grando, F. P.** and **Prata, A. T.** Computational modeling of oil-refrigerant two-phase flow with foam formation in straight horizontal pipes. In Proceedings of the 2nd International Conference on *Heat transfer, fluid mechanics and thermodynamics – HEFAT*, Zambia, 2003, paper GF2.

17 **Barbosa, Jr., J. R., Lacerda, V. T.,** and **Prata, A. T.** Prediction of pressure drop in refrigerant–lubricant oil flows with high contents of oil and refrigerant outgassing in small diameter tubes. *Int. J. Refrig.*, 2004, **27**, 129–139.

18 **Dowson, D.** and **Taylor, C. M.** Cavitation in bearings. *Annu. Rev. Fluid Mech.*, 1979, **11**, 35–66.

19 **Grando, F. P., Priest, M.,** and **Prata, A. T.** Lubrication in refrigeration systems: performance of journal bearings lubricated with oil and refrigerant mixtures. Life cycle tribology, Proceedings of the 31st Leeds-Lyon Symposium on *Tribology*, Leeds 2004, Tribology and Interface Engineering Series, 2005, pp. 481–491 (Elservier, Amsterdam).

20 **Grando, F. P., Priest, M.,** and **Prata, A. T.** A two-phase flow approach to cavitation modeling in journal bearings. *Tribol. Lett.*, 2006, in press, DOI: 10.1007/s11249-006-9027-6.

21 **Yokozeki, A.** Time-dependent behavior of gas absorption in lubricant oil. *Int. J. Refrig.*, 2002, **25**, 695–704.

22 **Silva, A.** *Kinetics and dynamics of gas absorption by lubricant oil*. DEng thesis, Federal University of Santa Catarina, Florianopolis, Brazil, 2004.

23 **Pinkus, O.** and **Sternlicht, B.** *Theory of hydrodynamic lubrication*, 1961 (McGraw-Hill, New York).

24 **Carey, V. P.** *Liquid–vapor phase-change phenomena*, 1992 (Hemisphere, New York).

25 **Patankar, S. V.** *Numerical heat transfer and fluid flow*, 1980 (McGraw-Hill, New York).

26 **Rigola, J., Perez-Segarra, C. D., Raush, G., Oliva, A., Escriba, M., Jover, J.,** and **Escanes, F.** Experimental studies of hermetic reciprocating compressors with special emphasis on pv diagrams. Proceedings of the 16th International Compressor Engineering Conference at Purdue, Purdue, USA, 2002, paper C4-1.

27 **Venner, C. H.** and **Lubrecht, A. A.** *Multilevels methods in lubrication*. Tribology Series 37, 2000 (Elsevier, Amsterdam)

28 **McLinden, M. O., Klein, S. A., Lemmon, E. W.,** and **Peskin, A. W.** REFPROP: Thermodynamic and transport properties of refrigerants and refrigerant mixtures, version 6.0. Washington (DC): NIST, 1998.

APPENDIX 1

Notation

A_P	piston axial acceleration (m/s^2)
c	radial clearance between piston and cylinder (m)
C_{BP}	distance between connecting rod centre of mass and the piston gudgeon pin (m)
C_{MB}	connecting rod length (m)
d	distance between the crankshaft centre and the cylinder axis, 'offset' (m)
e	eccentricity (m)
F_f	friction force (N)
F_g	force due to the compression of the gas (N)
F_h	hydrodynamic force (N)
F_{rx}	connecting rod force, direction x(N)
F_{rz}	connecting rod force, direction z(N)
h	lubricant film thickness (m) $= c - [e_t + (e_b - e_t)\xi R/L]\cos\theta$
I_P	moment of inertia of the piston about the gudgeon pin (kg m^2)

L	piston length (m)
m	mass of the piston (kg)
m_b	connecting rod mass (kg)
m_l	total mass of liquid (oil + refrigerant) (kg)
m_{lr}	mass of liquid refrigerant (kg)
M_f	moment due to viscous friction, in relation to the pin (N m)
M_h	hydrodynamic moment about the pin (N m)
p	absolute pressure (Pa)
P_{ot}	power consumption by viscous friction (W)
q_{bottom}	volumetric flow rate at the bottom of the piston (m^3/s)
r	radial coordinate (m)
R	piston radius (m)
t	time (s)
T	temperature (°C)
V_P	piston axial velocity (m/s)
w	refrigerant mass fraction (kg_{ref}/kg_{mixt})
w_o	overall refrigerant mass fraction (kg_{ref}/kg_{mixt})
w_r	mass fraction immediately before the instant considered (kg_{ref}/kg_{mixt})
w_{sat}	refrigerant solubility in the oil (kg_{ref}/kg_{mixt})
x	coordinate of the Cartesian system (m)
y	coordinate of the Cartesian system (m)
z	axial coordinate of the Cartesian system (m)
z_P	pin location from the top of the piston (m)

γ	axial coordinate for the polar system (m)
$\Delta\tau$	step in the crankshaft angle (rad, °)
ε	eccentricity ratio ($= e/c$) (–)
$\dot{\varepsilon}$	velocity in the radial direction (1/s)
$\ddot{\varepsilon}$	acceleration in the radial direction ($1/s^2$)
θ	angular coordinate, polar system (rad, °)
κ	coefficient of absorption (–)
μ	dynamic viscosity (Pa s)
$\bar{\mu}$	homogeneous viscosity, equation (7) (Pa s)
ξ	dimensionless axial coordinate ($=\gamma/R$) (–)
ρ	density (kg/m^3)
$\bar{\rho}$	homogeneous density, equation (6) (kg/m^3)
τ	crankshaft angle ($= \omega t$)(rad, °)
ø	void fraction, equation (5) (–)
χ	gas quality, equation (3) (kg/m^3)
ω	crankshaft angular velocity (rad/s)

Superscripts and subscripts

b	bottom of the piston
cyl	cylinder
CM	centre of mass
g	gas phase
l	liquid phase
mixt	mixture
ref	refrigerant
suc	at the suction or shell
t	top of the piston
τ	previous crankshaft position
$\tau+\Delta\tau$	current crankshaft position

APPENDIX 2: CALCULATION OF PHYSICAL PROPERTIES

Empiricism is the most common procedure in determining physical properties for oil–refrigerant mixtures, very often adjusting curves from experimental data that have been made available. In this work, properties for the mixture of refrigerant R134a and oil ICI EMKARATE RL10H were calculated using data provided in graphical form by the oil manufacturer. For pure refrigerant, data were obtained from the software REFPROP [**28**]. This section presents the numerical correlations adopted to calculate the physical properties required. Further discussion on the properties of the fluids and the behaviour of this specific mixture can be found by Silva [**22**].

A.1 Solubility

The solubility of R134a in the polyol ester oil ICI EMKARATE RL10H was provided by the oil manufacturer in a diagram and adjusted by curve fitting for the interval $0 < p < 1000$ kPa and $0 < T < 60$ °C as

$$w_{sat} = \frac{a_1 + b_1 p + c_1 T + d_1 p^2 + e_1 T^2 + f_1 Tp}{a_2 + b_2 p + c_2 T + d_2 p^2 + e_2 T^2 + f_2 Tp} \tag{23}$$

where $a_1 = 0.6825$, $b_1 = 0.0701$, $c_1 = 0.0699$, $d_1 = -1.2087 \times 10^{-4}$, $e_1 = -1.7157 \times 10^{-3}$, $f_1 = 2.4124 \times 10^{-3}$, $a_2 = 1.0$, $b_2 = -3.1315 \times 10^{-3}$, $c_2 = 0.0503$, $d_2 = 1.0541 \times 10^{-6}$, $e_2 = 1.3645 \times 10^{-3}$, $f_2 = -6.4074 \times 10^{-5}$.

A.2 Density

The density for the mixture R134a–EMKARATE RL10H is calculated using the additive law of mixtures. Considering an ideal mixture, the result is presented in the following equation

$$\rho_l = \frac{\rho_{oil}}{1 + w_r((\rho_{oil}/\rho_{lr}) - 1)} \tag{24}$$

where ρ_l is the density of the liquid mixture, ρ_{oil} the density of the pure oil, ρ_{lr} the density of the liquid refrigerant, and w_r is the refrigerant mass fraction.

The oil density provided by the manufacturer and adjusted in the range $20 < T < 120\,^{\circ}\text{C}$ is given by

$$\rho_{oil} = a_3 + b_3 T + c_3 T^2 \tag{25}$$

where $a_3 = 966.4364$, $b_3 = -0.5739$, $c_3 = -2.4476 \times 10^{-4}$, and ρ_{oil} the density in kg/m^3.

The density of the liquid refrigerant is obtained from the software REFPROP [**28**] and validated for the interval $-5 < T < 60\,^{\circ}\text{C}$ as follows

$$\rho_{lr} = a_4 + b_4 T + c_4 T^2 \tag{26}$$

where $a_4 = 1294.6790$, $b_4 = -3.2213$, $c_4 = -0.0123$, and ρ_{lr} the density in kg/m^3.

A.3 Dynamic viscosity

The viscosity of the liquid mixture R134a and the polyol ester oil was provided by the oil manufacturer and the following fit is proposed for the interval $0 < T < 60\,^{\circ}\text{C}$ and $0 < w_r < 1$

$$\mu_l = \frac{a_5 + b_5 T + c_5 w_r + d_5 T^2 + e_5 w_r^2 + f_5 T w_r}{a_6 + b_6 T + c_6 w_r + d_6 T^2 + e_6 w_r^2 + f_6 T w_r} \tag{27}$$

where $a_5 = 0.0371$, $b_5 = 9.1603 \times 10^{-5}$, $c_5 = -0.0800$, $d_5 = -2.7390 \times 10^{-7}$, $e_5 = -0.0435$, $f_5 = -6.0485 \times 10^{-5}$, $a_6 = 1.0$, $b_6 = 0.0531$, $c_6 = 2.2309$, $d_6 = 1.1656 \times 10^{-3}$, $e_6 = -0.3053$, $f_6 = 0.0334$, and μ_l the viscosity (Pa s).

A.4 Properties for the refrigerant in gas phase

The properties of the gas were obtained using the software REFPROP [**28**], and for the interval $0 < p < 1600$ kPa and $0 < T < 60\,^{\circ}\text{C}$ the following fits are proposed for density ρ_g (kg/m^3) and viscosity μ_g (Pa s), respectively

$$\rho_g = \frac{a_7 + b_7 p + c_7 T + d_7 p^2 + e_7 T^2 + f_7 T p}{a_8 + b_8 p + c_8 T + d_8 p^2 + e_8 T^2 + f_8 T p} \tag{28}$$

where $a_7 = 4.2473 \times 10^{-3}$, $b_7 = -1.9077 \times 10^{-4}$, $c_7 = 0.0448$, $d_7 = 3.4605 \times 10^{-5}$, $e_7 = -2.4624 \times 10^{-5}$, $f_7 = 5.3830 \times 10^{-4}$, $a_8 = 1.0$, $b_8 = 0.0155$, $c_8 = -8.2500 \times 10^{-4}$, $d_8 = 4.5680 \times 10^{-5}$, $e_8 = 6.9326 \times 10^{-8}$, $f_8 = -2.1388 \times 10^{-6}$

$$\mu_g = \frac{a_9 + b_9 p + c_9 T + d_9 T^2 + e_9 p^3}{a_{10} + b_{10} p + c_{10} p^2 + d_{10} T} \times 10^{-6} \tag{29}$$

where $a_9 = 10.8186$, $b_9 = -2.6052 \times 10^{-3}$, $c_9 = 0.1451$, $d_9 = 3.7658 \times 10^{-4}$, $e_9 = -2.0170 \times 10^{-7}$, $a_9 = 1.0$, $b_{10} = -2.1278 \times 10^{-4}$, $c_{10} = -7.752 \times 10^{-9}$, $d_{10} = 9.6695 \times 10^{-3}$.